

# Protection of Parallel Transmission Lines Using Wavelet Transform

A. H. Osman, *Student Member, IEEE*, and O. P. Malik, *Life Fellow, IEEE*

**Abstract**—A new scheme to enhance the solution of the problems associated with parallel transmission line protection is presented in this paper. The scheme depends on the three line voltages and the six line currents of the two parallel lines at each end. Fault detection, fault discrimination, and calculation of the phasors of the measured signals are done by using wavelet transform (WT). By comparing the magnitudes of the estimated current phasors of the corresponding phases on both lines, internal faults on the parallel lines can be identified. Also, by calculating the distance element of the phases on which a disturbance is detected and having a very small current difference magnitude can enhance and strengthen the scheme. Studies show that all types of faults at different loading conditions can be correctly identified in less than one cycle of the fundamental frequency.

**Index Terms**—Distance protection, parallel lines protection, wavelet transform.

## I. INTRODUCTION

**D**ISTANCE protection relaying algorithms are commonly applied for the protection of overhead transmission lines. Their operation is based on measuring the input impedances of the lines using the voltage and current signals at the relay location. The input impedance of a short-circuited line varies from zero for a fault at its input terminals to a finite value for a fault at its remote end, the value of the impedance increasing with the distance to the fault. This relaying technique can successfully be applied for single-circuit lines. However, when applied to parallel lines, the performance of the conventional distance relays is affected by the mutual coupling between the lines. The mutual inductance between pairs of conductors in the two lines is not the same and, therefore, emfs are produced in the conductors of one line by the currents in the conductors of the other line. As a result, the apparent input impedance of a line on which a fault is present is affected by load currents or currents being fed to the fault by a parallel healthy line and the operation of the distance relay can be affected.

A number of solutions have been proposed to solve the parallel lines protection problem [1]–[5]. Adaptive distance protection schemes were proposed in [1] in which a correction factor, based on the information of the surrounding system of the protected line under different operating conditions, was used in the impedance calculation. A proposed scheme based on traveling wave was investigated in [2]. In [3], a technique based on comparing of currents in the corresponding phases of the two lines to detect faults and discriminate between faulty and healthy

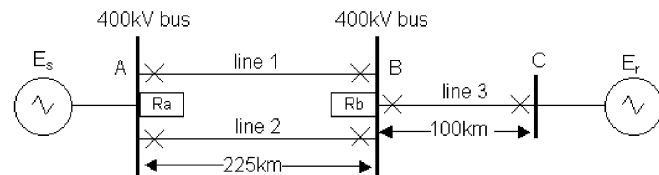


Fig. 1. Parallel transmission line model.

phases is proposed. In [4], phase currents comparison between the two circuits and positive sequence current level detection were used in conjunction with parallel line's zero sequence current compensated impedance calculation. In [5], a comparison between the measured impedance of corresponding phases was suggested.

A scheme based on using two relays one at each end of the parallel lines is proposed in this paper. Fig. 1 shows the parallel transmission line model and the location of the relays. All six current signals and three voltage signals on each end are needed for the proposed algorithm. Using wavelet transform (WT), it is easy to detect any disturbance or fault on the lines and to estimate the phasors of the measured signals [6]. The proposed algorithm is based on three stages. The first stage is the fast fault detection and phasors estimation using WT. The second stage is the comparison of the magnitudes of line currents in the corresponding phases of the two circuits. The third stage is the backup distance protection for some types of faults that current comparison cannot discriminate. Simulation studies illustrate the effectiveness of the scheme.

## II. WAVELET TRANSFORM

Wavelet transform was introduced at the beginning of the 1980s and has attracted much interest in the fields of speech and image processing since then. Its potential applications to power industry have been discussed recently [7], [8]. A brief introduction to the WT is given in Appendix A.

In this approach, any function  $f(t)$  can be expanded in terms of a class of orthogonal basis functions as described in Appendix A. In wavelet applications, different basis functions have been proposed and selected. Each basis function has its feasibility depending on the application requirements. In the proposed scheme, the Daubechies-4 (db4) wavelet with eight coefficients was selected after extensive comparison with other wavelets to serve as a wavelet basis function for the detection and estimation of the voltage and current phasors. Daubechies family is one of the most suitable wavelets in analyzing power system transients [9], [14]–[17].

Manuscript received August 13, 2002.

The authors are with the Department of Electrical and Computer Engineering, University of Calgary, Calgary, AB T2N 1N4, Canada  
Digital Object Identifier 10.1109/TPWRD.2003.820419

### III. PROPOSED ALGORITHM

The measured three voltages and six current signals (at each end) are filtered using preband-pass filters with center frequency of 60 Hz to attenuate the dc component. These nine signals are sampled at a sampling frequency of 960 Hz. The algorithm starts by collecting a one cycle sampled data window for each signal. Based on a sampling frequency of 960 Hz, one cycle contains 16 samples. For each new sample to enter the window, the oldest one is disregarded and the algorithm starts.

The algorithm depends on utilizing WT for its powerful analyzing and decomposing features. For each data window, the wavelet transform decomposes the signals into three levels of decomposition. From the first decomposition level for the six-line currents, the high-frequency components can be extracted from the signal and a disturbance can be detected by observing the norm of the detail coefficients D1 (Appendix A). If the norm of D1 for each line current is less than a certain threshold ( $M$ ), this means that the lines are healthy.

Theoretically, the phasors should be estimated from the third decomposition level (0–60 Hz). Since the compact support wavelets do not have ideal cut-off frequency characteristics, the phasors cannot be obtained from this level. It is essential to use some margins on both sides of the frequency of interest. Therefore, the fundamental frequency (60 Hz) falls into the middle of the approximation output of the second level. From the second level of decomposition (0–120 Hz), the phasor (magnitude and angle) of each signal can be estimated by using the approximation coefficients vector of A2 (Appendix A). Using these phasors, the sequence components of the currents of both lines can be calculated.

For each new sample, a check is performed for the case of one line being disconnected. This can be done by observing the level of the positive sequence current magnitude of both lines. If one line is disconnected, an alternative algorithm for single-line distance protection should be executed [6].

Once the norm of one or more current detail coefficients exceeds the threshold ( $M$ ), a disturbance is detected. A new data window ( $n_w$ ) is started from the sample at which the disturbance has been detected. Each time a new sample enters the window, the phasors of all current and all voltage signals are estimated and the difference ( $I_{diff}$ ) between the phasor magnitudes of the currents of the corresponding phases, on which the WT has detected a disturbance, is calculated. For example, the difference between the magnitudes of currents of phase “a” corresponding phasors is

$$I_{aDiff} = |I_{a1}| - |I_{a2}|.$$

If the difference is above a predetermined positive threshold level ( $L$ ), a trip signal should be sent to the circuit breaker of line 1. If the difference is less than the negative value of ( $L$ ), a trip signal should be sent to the circuit breaker of line 2. If the difference is within the  $\pm L$  range, the distance relay will calculate the impedance(s) of the line(s) on which the WT detected a disturbance. According to the calculated impedance, the disturbance will be classified as a fault on the line (internal or external) or a disturbance that happened for any other reason. If the disturbance is classified as a fault on the line, the distance relay will

determine the zone of the fault and trip the circuit breaker according to its time delay.

When the number of samples ( $n_w$ ) collected after detecting a disturbance reaches 16, the oldest sample in the window is disregarded when a new one enters the data window. The algorithm will continue with the same procedure and with 16-sample data window for two more cycles. If no fault is detected, the algorithm will start again from the beginning. A flowchart for the proposed parallel-lines protection algorithm is shown in Fig. 2.

The advantage of using only new samples in the data window after the inception of a disturbance is to accelerate the identification of the fault whether it is internal or external. If the window contains both old and new data samples, the identification process will experience delay. The calculated impedances for ground faults are based on deriving the positive-, negative-, and zero-sequence current values from the estimated phasors of only the line on fault.

A compensation for the mutual coupling between lines is not included because this compensation may lead to a first zone tripping for faults beyond the remote end of the parallel lines. Such over-reach is not acceptable and it is therefore much more serious than the under reach, which can occur without compensation for the mutual coupling [10]. The first zone reach is set to 90% of the line positive sequence impedance. The equations used in calculating the impedances of ground and phase faults are shown in Appendix B.

The value of the threshold  $M$  used to detect disturbances by monitoring the norm of D1, is chosen based on extensive simulations on the parallel lines model for all types of faults and loading conditions being studied. It has been found that under all normal loading conditions,  $M$  is less than 0.3. A value of 0.4 is assigned for  $M$  to increase the detection sensitivity.

The threshold  $L$ , used to detect the abnormal difference in the current magnitude of the corresponding phases on both lines is chosen carefully to achieve a secure response. For faults on the parallel lines  $L$  should exceed  $\pm 20\%$  of the maximum load current during normal loading conditions. If the difference is less than this value, this implies that the disturbance detected is either an external fault or an error due to the difference in current transformers characteristics and a certain inequality in the primary currents.

### IV. SIMULATION STUDIES

The model network shown in Fig. 1 has been simulated using PSCAD program. The network consists of two areas connected by two sections of 400-kV transmission lines. The first section AB contains two 225-km-long parallel lines, and the second section BC is equivalent to a 100-km line. Each of the parallel lines has a zero sequence impedance  $Z_{L0} = 81.32 + j310.48$  (ohms); and positive sequence impedance  $Z_{L1} = 8.16 + j108.82$  (ohms). The source voltages are  $E_s = 400$  kV and  $E_r = 400\angle\delta$  kV, where  $\delta$  is the load angle in degrees.

To ensure the isolation of faults, similar relays are provided at each end of the line. All three-line voltage signals and all six-line current signals at both ends (A and B) of the parallel lines are passed through bandpass filters with a center frequency of 60

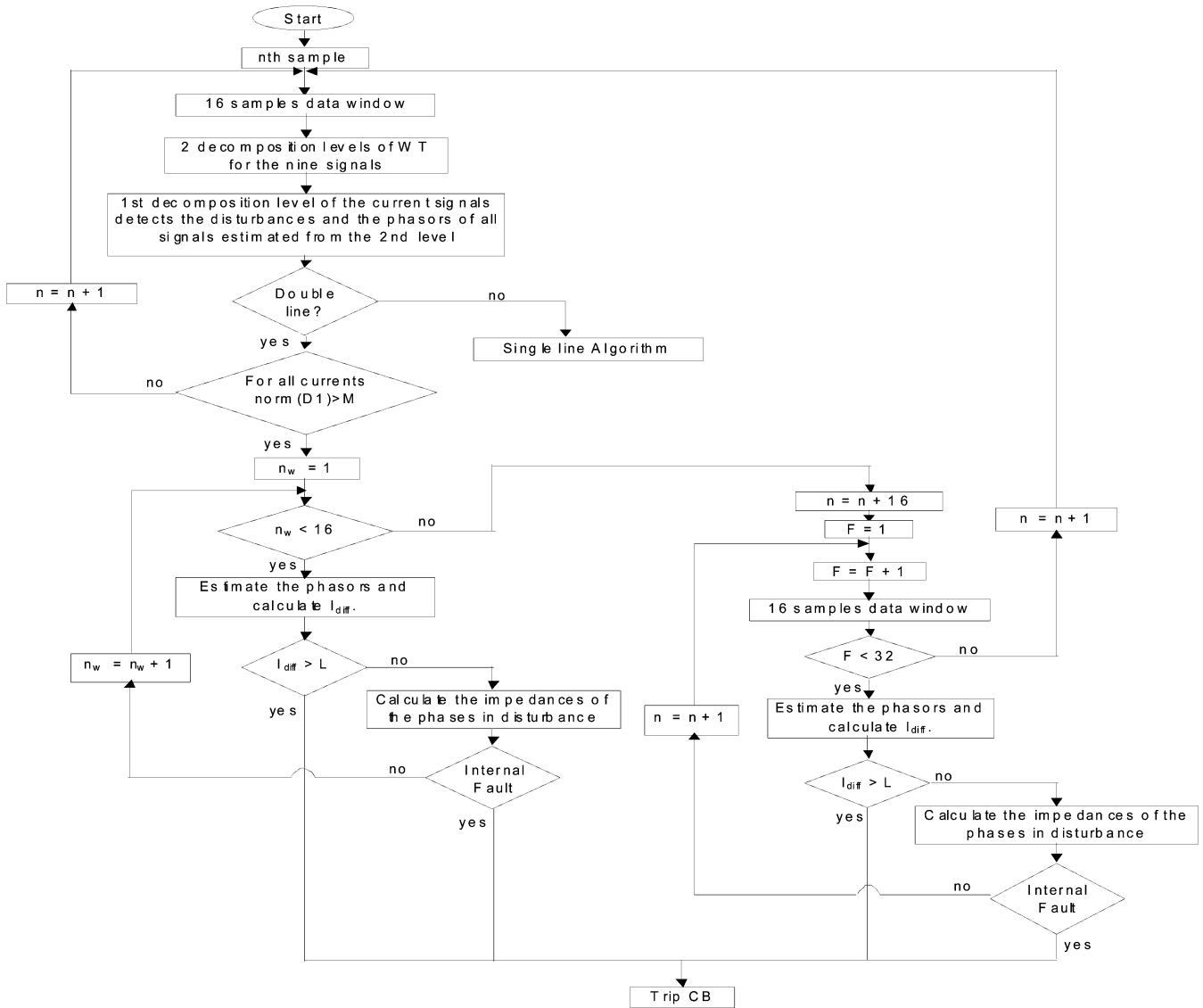


Fig. 2. Proposed parallel lines protection algorithm.

Hz. The signals are then sampled at a sampling frequency of 960 Hz. These sampled signals perform as the inputs to the WT protection algorithm. The described WT algorithm is applied and tested on the model network. The tests include solid and resistive ground faults, phase and intercircuit faults, at different locations and different loading conditions, and also for external faults. All simulations are done for the relay at bus A.

A. Single Line Faults

A solid single line to ground fault (SLG) is applied on phase “a” of line 1 at 100 km from the relay at bus A and with a load angle  $\delta = -15^\circ$ . Fig. 3 shows the process of disturbance detection using WT. It is clear that only the norm of the WT first level detail coefficients of phase “a” of line 1 exceeded the detection level ( $M$ ). Fig. 4 shows ( $I_{aDiff}$ ), the difference in the corresponding line currents of phase “a” on which the WT detected a disturbance. This difference is calculated using the magnitudes of the phasors, which are estimated from the second level approximations of the WT. Since  $I_{aDiff}$  has a positive value, the

fault is known to be on phase “a” of line 1. The figure also shows the trip signal, which is launched four samples after ( $I_{aDiff}$ ) exceeded the current difference threshold ( $L$ ) for reliability and security.

A SLG fault with high ground fault resistance ( $50 \Omega$ ) is applied on phase “c” of line 2 at 150 km from bus A and with a load angle  $\delta = -20^\circ$ . Like the previous case, the norm of the WT first level detail coefficients exceeded the threshold value ( $M$ ) and, thus, the difference of the corresponding line current phasors magnitudes of phase “c” ( $I_{cDiff}$ ) is calculated. Fig. 5 shows  $I_{cDiff}$  exceeded the current difference threshold ( $L$ ), and the trip signal after four samples. It is obvious that high ground faults can be easily identified.

B. Line-to-Line Fault

The relay has been tested for line-to-line faults on one of the two parallel lines.

The current difference magnitudes ( $I_{aDiff}$ ), ( $I_{bDiff}$ ) and the trip signal for a double line fault (a-b) on line 1 at 120 km from

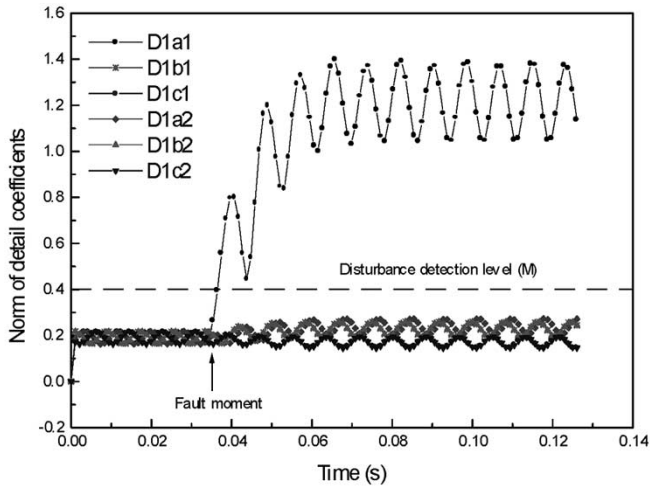


Fig. 3. Norm of WT first level detail coefficients of all line currents for SLG at 100 km from bus A.

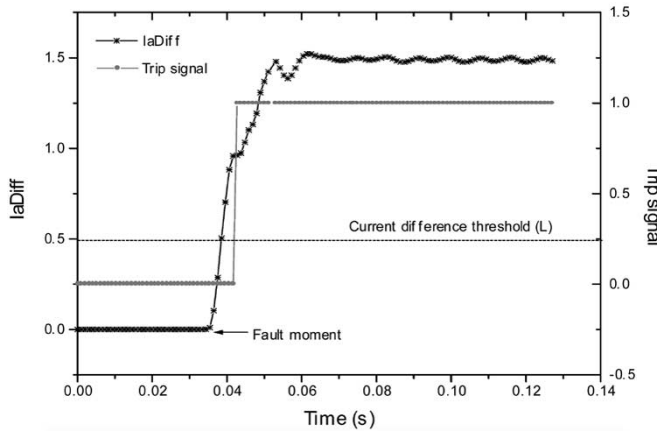


Fig. 4.  $I_{aDiff}$  and trip signal of SLG fault at 100 km from bus A.

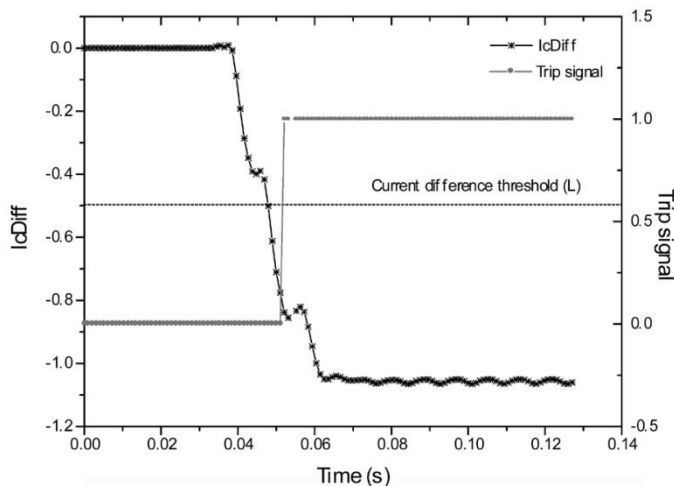


Fig. 5.  $I_{cDiff}$  and trip signal of a SLG fault on line 2 at 150 km with 50- $\Omega$  fault resistance.

the relay at bus A and with a load angle of  $\delta = 20^\circ$  are shown in Fig. 6. This fault will cause a three-phase trip only for line 1.

### C. Simultaneous Fault on Both Lines

The current difference magnitudes ( $I_{aDiff}$ ), ( $I_{bDiff}$ ), and the trip signal for a phase “a” to ground fault on line 1 and a phase

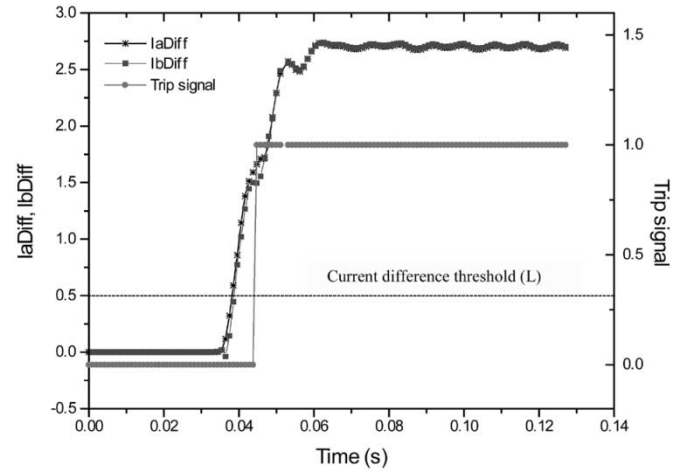


Fig. 6.  $I_{aDiff}$ ,  $I_{bDiff}$ , and the trip signal for DL fault on line 1 at 120 km from bus A.

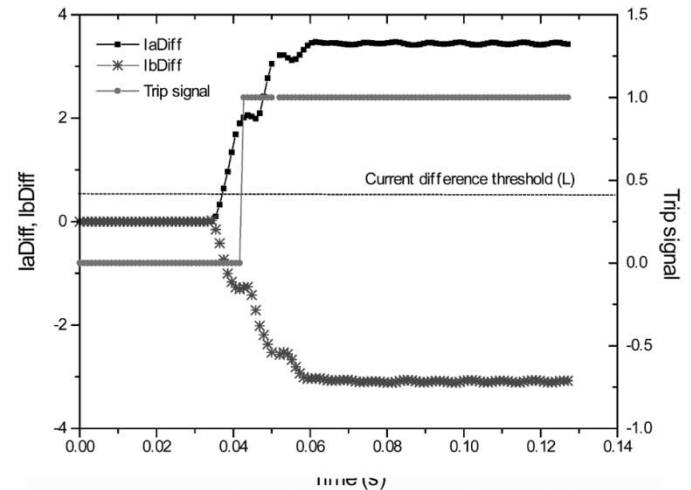


Fig. 7.  $I_{aDiff}$ ,  $I_{bDiff}$ , and trip signal for “a-G” on line 1 and “b-G” on line 2 at 100 km from bus A.

“b” to ground fault on line 2 (cross country fault) are shown in Fig. 7. The fault is applied at 100 km from the relay at bus A, and at a load angle  $\delta = -20^\circ$ . This type of fault is difficult to be identified when only distance relaying is employed to protect the parallel lines. The distance relay will identify this fault as a double line to ground fault on both lines and a three-phase tripping signal will be sent to the circuit breakers of both lines [5]. It can be seen that using this technique, the fault is correctly identified and a single-pole tripping signal for the phase on fault in each line will be sent to its circuit breaker.

Fig. 8 shows the detection of a very special fault case when a line to ground fault occurs on one phase of line 1 and, at the same time, the corresponding phase on line 2 has the same type of fault. In this case, the fault is “a-G” on line 1 and “a-G” on line 2 at 100 km from the relay at bus A and at a load angle  $\delta = -30^\circ$ . It can be realized that the WT detected a disturbance only in phase “a” of both lines. For this type of fault, the current difference technique or the impedance difference technique will not notice the fault because the difference is almost zero. If the difference between the corresponding line currents of these phases is small or zero, a backup distance measurement based on the estimated phasors of the signals is done.

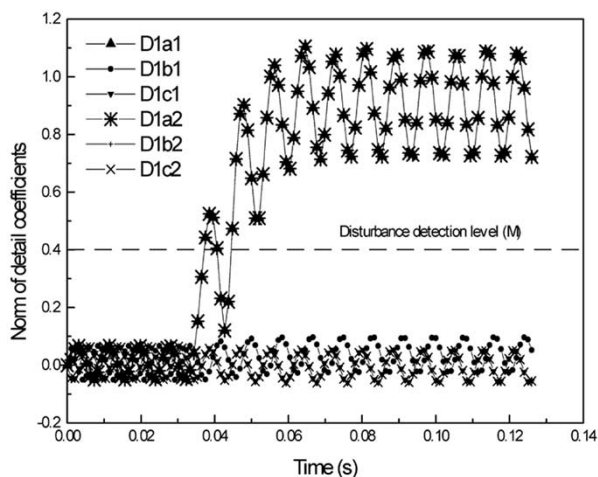


Fig. 8. Norm of WT first level detail coefficients of all line currents for “a-G” on line 1 and “a-G” on line 2 at 100 km from bus A.

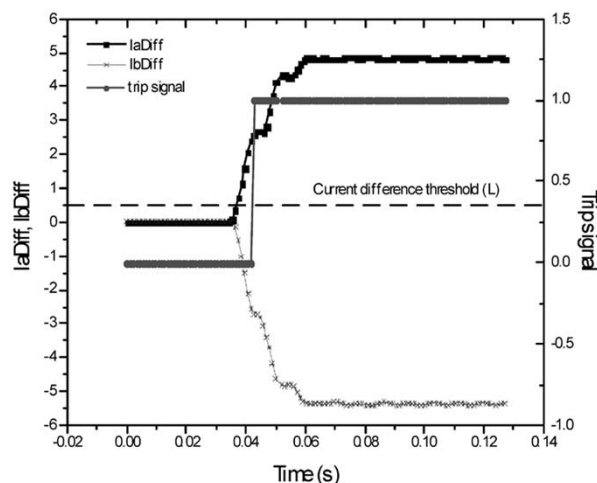


Fig. 10.  $I_{aDiff}$ ,  $I_{bDiff}$ , and trip signal for a clashing fault between phase “a” on one circuit and phase “b” on the other circuits at 50 km.

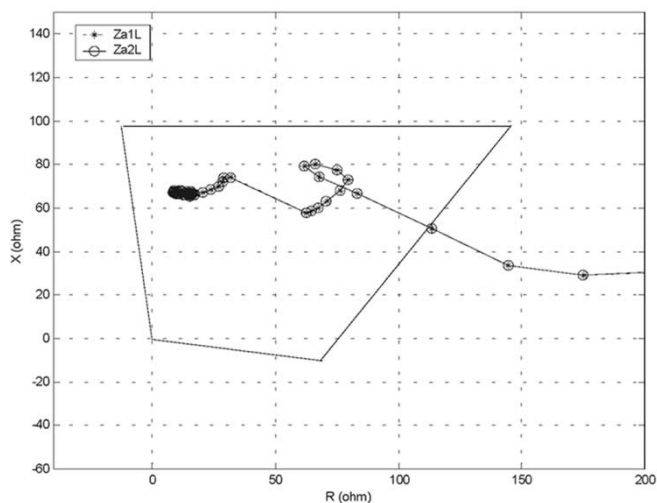


Fig. 9. Impedance trajectory for SLG “a-G” on line 1 and SLG “a-G” on line 2 at 100 km from bus A.

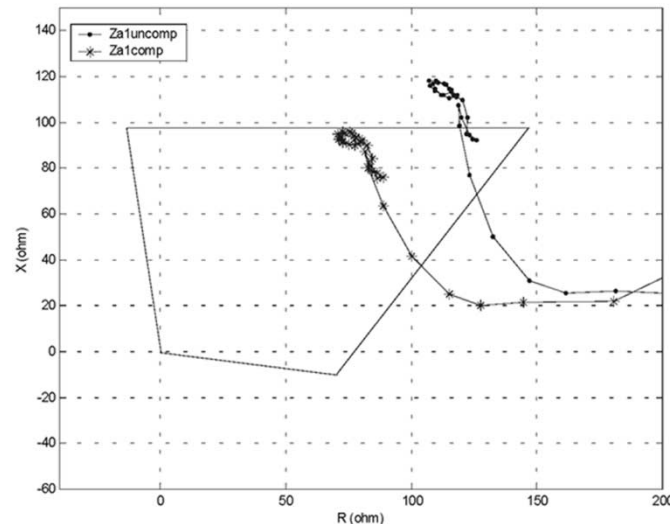


Fig. 11. Impedance trajectories with and without mutual coupling for an SLG “a-G” at the remote end.

The distance algorithm will calculate the impedances corresponding to the fault location and according to the fault type detected from the phases subject to the disturbance. This backup helps to detect same phase faults (i.e., simultaneous fault between phase “a” and ground on line 1, and between phase “a” and ground on line 2). The ground impedance trajectories of phase “a” on both lines are shown in Fig. 9. Since the fault occurred at the same distance on both lines, the impedance trajectories are almost the same and as shown in Fig. 9 they are superimposed. The distance measurement does not include a compensation for the mutual coupling between lines in order to avoid the over-reach in the case of a fault beyond the remote end [10].

The proposed technique has been also tested for a phase-to-phase clashing conductors fault. Fig. 10 shows the current difference magnitudes ( $I_{aDiff}$ ), ( $I_{bDiff}$ ) and the trip signal for a phase “a” of line 1 to phase “b” of line 2 clashing conductors fault at 50 km from the relay at bus A and with a load angle of  $\delta = 20^\circ$ . The trip signal is launched after four samples the current difference magnitudes ( $I_{aDiff}$ ) and ( $I_{bDiff}$ ) exceeded the current difference threshold ( $L$ ).

#### D. External Faults

In the case of external faults, WT provides the ability to detect the disturbance occurring in the related phase(s). The current difference in the corresponding phases is almost zero and, thus, the algorithm will move to the distance line protection algorithm. This case here demonstrates the importance of having a distance protection algorithm working as a backup for the current difference algorithm.

A SLG “a-G” fault is applied at the remote end of the line with ground fault resistance of  $30 \Omega$  and load angle  $\delta = 30^\circ$ . WT detected a disturbance in phase “a” on both lines. The calculated ground impedances for phase “a” on both lines are equal. Only the impedance of line 1 will be considered here. Fig. 11 shows the impedance trajectory seen by the relay at bus A of line 1 with and without mutual coupling compensation. It is clear that the compensation for the mutual coupling leads the calculated impedance  $Z_{a1comp}$  to settle in the first protection zone and give false trip on both lines. On the other hand, the calculated impedance  $Z_{a1uncomp}$  without coupling compensation

settles outside the first zone and the relay performs as a backup for the protection of the adjacent line.

## V. CONCLUSION

A new scheme for the protection of parallel lines is presented in this paper. The scheme depends on measuring all current and voltage signals at both ends of the parallel lines. The WT with its magnificent characteristics is employed to detect the disturbances in the current signals and to estimate the phasors of all the signals as well as to achieve high-speed relaying. The difference in the current phasor magnitudes of the phase on which the fault is detected and of the corresponding phase on the other line is calculated, and the line with the higher magnitude is isolated. In some cases, the current difference technique is not enough to protect parallel lines. In these cases, the distance algorithm should be applied in order to have protection coverage for all types of faults. The relay has been successfully tested for all types of faults at different locations and loading. All faults are identified in less than one cycle after the fault inception.

## APPENDIX A

### A. WT—Introduction

A brief introduction to the wavelet transform is given here. More details can be found in [11] and [12]. There are two fundamental equations upon which wavelet calculations are based; the scaling function  $\varphi(t)$  and the wavelet function  $\Psi(t)$

$$\varphi(t) = \sqrt{2} \sum_k h_k \varphi(2t - k) \quad (1)$$

$$\psi(t) = \sqrt{2} \sum_k g_k \varphi(2t - k). \quad (2)$$

These functions are two-scale difference equations based on a chosen scaling function  $\varphi$ , with properties that satisfy certain admission criteria. The discrete sequences  $h_k$  and  $g_k$  represent discrete filters that solve each equation. The scaling and wavelet functions are the prototype of a class of orthonormal basis functions of the form

$$\varphi_{j,k}(t) = 2^{j/2} \varphi(2^j t - k) \quad j, k \in \mathbb{Z} \quad (3)$$

$$\psi_{j,k}(t) = 2^{j/2} \psi(2^j t - k) \quad j, k \in \mathbb{Z} \quad (4)$$

where the parameter  $j$  controls the dilation or compression of the function in time scale and amplitude, the parameter  $k$  controls the translation of the function in time, and  $\mathbb{Z}$  is a set of integers.

Once a wavelet system is created, it can be used to expand a function  $f(t)$  in terms of the basis functions

$$f(t) = \sum_{l \in \mathbb{Z}} c(l) \varphi_l(t) + \sum_{j=0}^{J-1} \sum_{k \in \mathbb{Z}} d(j, k) \psi_{j,k}(t) \quad (5)$$

where the coefficients  $c(l)$  and  $d(j, k)$  are calculated by inner product as

$$c(l) = \langle \varphi_l | f \rangle = \int f(t) \varphi_l(t) dt \quad (6)$$

$$d(j, k) = \langle \psi_{j,k} | f \rangle = \int f(t) \psi_{j,k}(t) dt. \quad (7)$$

The expansion coefficients  $c(l)$  represent the approximation of the original signal  $f(t)$  with a resolution of one point per every

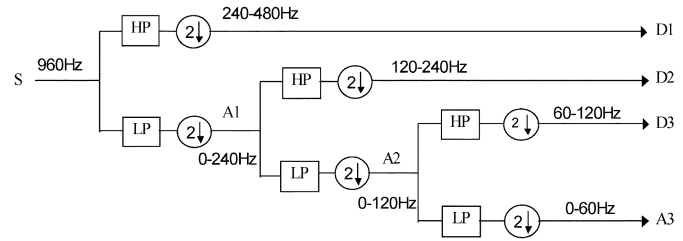


Fig. 12. WT multiresolution algorithm.

$2^J$  points of the original signal. The expansion coefficients  $d(j, k)$  represent details of the original signal at different levels of resolution.  $c(l)$  and  $d(j, k)$  terms can be calculated by direct convolution of  $f(t)$  samples with the coefficients  $h_k$  and  $g_k$ .

The wavelet transform can be implemented with a specially designed pair of finite impulse response (FIR) filters called a “quadrature mirror filters” (QMFs) pair. QMFs are distinctive because the frequency responses of the two FIR filters separate the high-frequency and low-frequency components of the input signal. The dividing point is usually halfway between 0 Hz and half the data sampling rate (the Nyquist frequency).

The outputs of the QMF filter pair are decimated (or desampled) by a factor of two. The low-frequency (low-pass) filter output is fed into another identical QMF filter pair. This operation can be repeated recursively as a tree or pyramid algorithm, yielding a group of signals that divides the spectrum of the original signal into octave bands with successively coarser measurements in time as the width of each spectral band narrows and decreases in frequency. The tree or pyramid algorithm can be applied to the wavelet transform by using the wavelet coefficients as the filter coefficients of the QMF filter pairs as shown in [13]. The same wavelet coefficients are used in both low-pass (LP) and high-pass (HP) filters. The LP filter coefficients are associated with the  $h_k$  of the scaling function  $\phi(t)$  and the HP filter is associated with the  $g_k$  of the wavelet function  $\Psi(t)$ . Fig. 12 shows the tree algorithm of a multiresolution WT for a signal  $S$ . The outputs of the LP filters are called the approximations (A), and the outputs of the HP filters are called the details (D).

### B. Phasors Estimation

The phasors of the measured voltage and current signals at the fundamental frequency can be estimated by using a unity amplitude 60-Hz sinusoidal reference signal (R1), sampled at the same sampling rate as the measured signals (960 Hz). For each data window, the sinusoidal reference signal and the measured signals are decomposed into two levels of decomposition using “db4” mother wavelet. As aforementioned, the phasors are estimated from the approximate coefficients A2 vector of the second decomposition level. The magnitude and angle with respect to the reference sinusoidal signal for each measured signal can be estimated using the basic vector mathematics. For example, if the approximate coefficients A2 vector of the second decomposition level of the sinusoidal reference is  $A_{2R1}$  and for one of the measured signals (S) is  $A_{2S}$ , then the angle  $\theta$  between the two vectors is defined as

$$\theta = \cos^{-1} \frac{(A_{2R1} \cdot A_{2S})}{|A_{2R1}| |A_{2S}|}$$

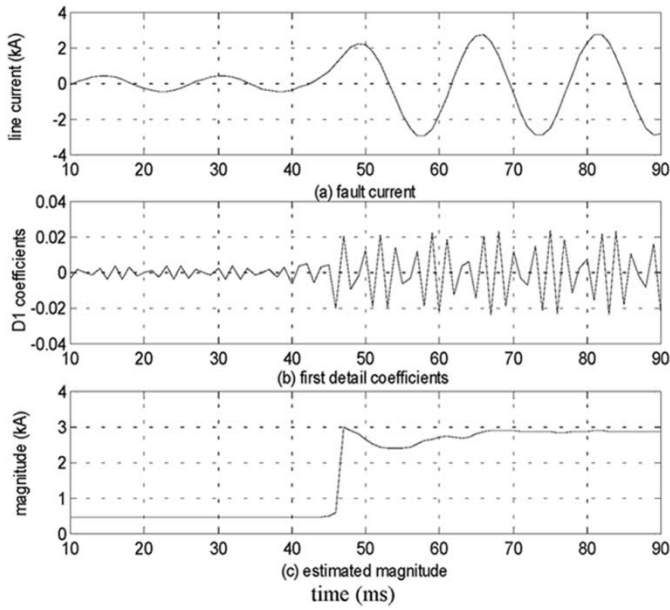


Fig. 13. Fault current signal with its first detail coefficients and its estimated magnitude.

where  $(A_{2R1} \cdot A_{2S})$  is the dot product of the two vectors and  $|A_{2R1}|$ ,  $|A_{2S}|$  are the norms of the two vectors.

A new unity amplitude sinusoidal signal (R2) with a phase shift equal to the calculated angle  $\theta$  is constructed and sampled at the same previous sampling frequency. The new signal is then decomposed into two decomposition levels using the same mother wavelet as used before. Using the second approximate coefficient vector  $A_{2R2}$  of this constructed sinusoidal signal, and the second approximate coefficient vector  $A_{2S}$  of the measured signal, the magnitude  $X$  of the measured signal can be defined as

$$X = \frac{|1||A_{2S}|}{|A_{2R2}|}$$

where  $|A_{2R2}|$  and  $|A_{2S}|$  are the norms of the second approximate coefficient vectors of the constructed and measured signals. The same procedure can be done for all the other measured signals to estimate their phasors.

Fig. 13 shows an example of a fault current signal decomposed using WT. The figure depicts the fault current signal, below which the first decomposition detail coefficients D1 for detecting disturbances and the magnitude estimated, respectively.

## APPENDIX B

### A. Impedance Calculation

For phase-to-ground faults

$$Z_{\text{phase}} = \frac{V_{\text{phase}}}{I_{\text{phase}}(1) + I_{\text{phase}}(2) + K(0)I_{\text{phase}}(0)}$$

$$K(0) = \frac{Z_L(0)}{Z_L(1)}$$

where  $V_{\text{phase}}$  is the estimated phase voltage phasor,  $I_{\text{phase}}(1)$ ,  $I_{\text{phase}}(2)$ , and  $I_{\text{phase}}(0)$  are the positive-, negative-, and zero-sequence components of estimated phase currents, respectively,

and  $K(0)$  is the ratio between the zero sequence to the positive sequence impedance of the protected transmission line.

For phase faults (example: phase "a" to phase "b" fault)

$$Z_{ab} = \frac{V_a - V_b}{I_a - I_b}$$

where  $V_a$  and  $V_b$  are the estimated voltage phasors,  $I_a$  and  $I_b$  are the estimated current phasors.

## REFERENCES

- [1] A. G. Jongepier and L. van der Sluis, "Adaptive distance protection of a double-circuit line," *IEEE Trans. Power Delivery*, vol. 9, pp. 1289–1295, July 1994.
- [2] M. H. J. Bollen, "Traveling-wave-based protection of double-circuit lines," *Proc. Inst. Elect. Eng. C*, vol. 140, no. 1, pp. 37–47, Jan. 1993.
- [3] M. I. Gilany, O. P. Malik, and G. S. Hope, "A digital technique for parallel transmission lines using a single relay at each end," *IEEE Trans. Power Delivery*, vol. 7, pp. 118–123, Jan. 1992.
- [4] P. G. McLaren, I. Fernando, H. Liu, E. Dirks, G. W. Swift, and C. Steele, "Enhanced double circuit line protection," *IEEE Trans. Power Delivery*, vol. 12, pp. 1100–1108, July 1997.
- [5] M. M. Eissa and M. Masoud, "A novel digital distance relaying technique for transmission line protection," *IEEE Trans. Power Delivery*, vol. 16, pp. 380–384, July 2001.
- [6] A. Osman and O. P. Malik, "Wavelet transform approach to distance protection of transmission lines," in *Proc. Power Eng. Soc. Summer Meeting*, Vancouver, BC, Canada, 2001.
- [7] D. Wai and X. Yibin, "A novel technique for high impedance fault identification," *IEEE Trans. Power Delivery*, vol. 13, pp. 738–744, July 1998.
- [8] D. C. Robertson, O. I. Camps, J. S. Mayer, and W. B. Gish, "Wavelet and electromagnetic power system transients," *IEEE Trans. Power Delivery*, vol. 11, pp. 1050–1056, Apr. 1996.
- [9] C. Kim and R. Aggarwal, "Wavelet transform in power systems," *Inst. Elect. Eng. Power Eng. J.*, vol. 15, no. 4, pp. 193–202, Aug. 2001.
- [10] E. B. Davison and A. Wright, "Some factors affecting the accuracy of distance type protective equipment under earth fault conditions," *Proc. Inst. Elect. Eng.*, vol. 110, pp. 1678–1688, 1963.
- [11] G. Strang and T. Nguyen, *Wavelet and Filter Banks*. Cambridge, MA: Wellesley-Cambridge, 1997.
- [12] C. S. Burrus and R. A. Gopinath, *Introduction to Wavelets and Wavelet Transforms a Primer*. Englewood Cliffs, NJ: Prentice-Hall, 1998.
- [13] S. G. Mallat, "A theory for multiresolution signal decomposition: The wavelet representation," *IEEE Trans. Pattern Anal. Mach. Intell.*, vol. 11, pp. 674–693, July 1989.
- [14] W. A. Wilkinson and M. D. Cox, "Discrete wavelet analysis of power system transients," *IEEE Trans. Power Syst.*, vol. 11, pp. 2038–2044, Nov. 1996.
- [15] T. B. Litter and D. J. Morrow, "Wavelets for the analysis and compression of power system disturbances," *IEEE Trans. Power Delivery*, vol. 14, pp. 358–364, Apr. 1999.
- [16] H. T. Yang and C. C. Liao, "A de-noising scheme for enhancing wavelet-based power quality monitoring system," *IEEE Trans. Power Delivery*, vol. 16, pp. 353–360, July 2001.
- [17] A. P. Meliopoulos and C. H. Lee, "An alternative method for transient analysis via wavelets," *IEEE Trans. Power Delivery*, vol. 15, pp. 114–121, Jan. 2000.

**A. H. Osman** (S'01) received the B.Sc. and M.Sc. degrees in electrical engineering from Helwan University, Cairo, Egypt, in 1991 and 1996, respectively. He is currently pursuing the Ph.D. degree at the University of Calgary, Calgary, AB, Canada.

His areas of interest include power system engineering, digital protection relaying, and power electronics.

**O. P. Malik** (M'66–SM'69–F'87–LF'00) graduated in electrical engineering from Delhi Polytechnic, Delhi, India, in 1952, and received the M.E. degree in electrical machine design from the University of Roorkee, Roorkee, India, in 1962. He received the Ph.D. degree from the University of London, London, U.K., in 1965 and the Diploma of the Membership of Imperial College from the Imperial College of Science and Technology, London, U.K., in 1966.

Currently, he is Faculty Professor Emeritus at the University of Calgary, Calgary, AB, Canada, where he has been since 1974.

Dr. Malik is a Fellow of the Institution of Electrical Engineers, U.K.